Astronomy
&
Astrophysics

APEX 1 mm line survey of the Orion Bar

S. Leurini[1], R. Rolffs[1], S. Thorwirth[1], B. Parise[1], P. Schilke[1], C. Comito[1], F. Wyrowski[1], R. Güsten[1], P. Bergman[2], K. M. Menten[1], and L.-Å. Nyman[2]

[1] Max-Planck-Institut für Radioastronomie, Auf dem Hügel 69, 53121 Bonn, Germany
  e-mail: sleurini@mpifr-bonn.mpg.de
[2] European Southern Observatory, Casilla 19001, Santiago, Chile

ABSTRACT

Context. Unbiased molecular line surveys are a powerful tool for analyzing the physical and chemical parameters of astronomical objects and are the only means for obtaining a complete view of the molecular inventory for a given source. The present work stands for the first such investigation of a photon-dominated region.

Aims. The first results of an ongoing millimeter-wave survey obtained towards the Orion Bar are reported.

Methods. The APEX telescope in combination with the APEX-2A facility receiver was employed in this investigation.

Results. We derived the physical parameters of the gas through LVG analyses of the methanol and formaldehyde data. Information on the sulfur and deuterium chemistry of photon-dominated regions is obtained from detections of several sulfur-bearing molecules and DCN.

Key words. ISM: individual objects: Orion Bar – ISM: abundances – ISM: molecules

1. Introduction

Photon-dominated regions (PDRs) are commonly found interstellar environments whose global properties are determined by intense far-ultraviolet (FUV) radiation emerging from nearby young OB stars (e.g. Hollenbach & Tielens 1997). Owing to its proximity and nearly edge-on orientation, the Orion Bar PDR has received particular attention as a template for studies of the spatial stratification of various atomic and molecular species from the highly penetrated surface layers deep into the parental molecular cloud. Targeted (sub)millimeter-wave investigations indicate that, besides a considerable number of ubiquitous astronomical molecules such as CO, CS, HCN, CH_3OH, and H_2CO, other species can be found that are suggestive of a unique PDR chemistry (Hogerheijde et al. 1995; Jansen et al. 1995; Fuente et al. 2003). One such example is the molecular ion CO^+ (e.g. Störzer et al. 1995), and another one appears to be CF^+, which so far has only been detected toward the Orion Bar (Neufeld et al. 2006, this volume). PDRs are also thought to show enhanced abundances of molecules carrying refractory elements due to grain breakup caused by the FUV radiation field (Schilke et al. 2001). Additionally, observations of the Horsehead nebula suggest that at least part of the molecular carbon chain budget in PDRs may be produced from UV-destruction of PAHs and carbonaceous grains (Pety et al. 2005).

In view of this, PDRs are attractive targets for unbiased molecular line studies, which also help to derive the global picture of the physics and chemistry associated with them. Here, we present the initial results from an unbiased molecular line survey obtained between 279 and 308 GHz with the APEX telescope (Güsten et al. 2006, this volume).

2. Observation

Observations were conducted with the APEX 12-m telescope[1] towards the Orion Bar at the position $\alpha_{2000} = 5^h35^m25.3^s$, $\delta_{2000} = -5°24'34.0''$, corresponding to the "Orion Bar (HCN)" position of Schilke et al. (2001), the most massive clump seen in $H^{13}CN$ (Lis & Schilke 2003, hereafter LS03). Data were taken in 2005, between October and December in the position-switching mode, with the reference position at (600'', 0''). The APEX-2A receiver (Risacher et al. 2006, this volume) was used in combination with the Fast Fourier Transform Spectrometer (Klein et al. 2006, this volume) providing a bandwidth of 1 GHz and a resolution of 0.12 km s^{-1}. The frequency range between 279 and 307.7 GHz was completely covered; additional data were taken in selected frequency ranges from 318.5 GHz to 361.5 GHz. Step-widths of approximately 500 MHz were used to cover each frequency setup twice to facilitate the side-band assignment. The antenna temperature was converted to the main-beam brightness temperature by using forward and beam efficiencies of 0.97 and 0.74, respectively. The noise level is of the order of 0.06 K–0.1 K, and the system temperature around 160 K. The calibration was performed by using the APECS software (Muders et al. 2006, this volume). The pointing was checked on Mars and was found to be accurate within a few arc-seconds. We estimate a calibration uncertainty of ~30%.

---

[1] This publication is based on data acquired with the Atacama Pathfinder Experiment (APEX). APEX is a collaboration between the Max-Planck-Institut für Radioastronomie, the European Southern Observatory, and the Onsala Space Observatory.

3. Analysis of the data

The line identification was based on the Cologne Database for Molecular Spectroscopy[2] (Müller et al. 2001) and on the JPL[3] (Pickett et al. 1998) line catalog and performed with the XCLASS software. We identified 16 different species and a number of their isotopologs; no strong unidentified lines were found in the range surveyed. In the following paragraphs, we focus on the excitation conditions of methanol (CH_3OH) and formaldehyde (H_2CO), on the one hand, and on the analysis of S-bearing molecules, on the other. Methanol and formaldehyde are present in our dataset with a large number of transitions (Table 1), and their collisional rates are available (Green 1991; Pottage et al. 2002). Thus, a more rigorous multi-line analysis is possible for these two species, which delivers temperature and density estimates. As for the S-bearing molecules in our dataset, some of them, namely CS, H_2S, SO, SO^+, and SO_2, have already been studied towards this source (Hogerheijde et al. 1995; Jansen et al. 1995; Fuente et al. 2003), whereas HCS^+, H_2CS and NS are being analyzed here for the first time in this environment. A comprehensive analysis will be presented once the line survey has been completed.

3.1. CH_3OH and H_2CO

The excitation analysis of CH_3OH and H_2CO was performed by using the method described by Leurini et al. (2004), recently modified to treat H_2CO as well. The procedure is based on the simultaneous fit of all the lines with a synthetic spectrum computed in the LVG approximation with the cosmic background as the only external radiation field. If lines are optically thick, the model fits source size, temperature, H_2 density, and CH_3OH/H_2CO column density; for optically thin lines, source size and column density cannot be determined independently, and beam-averaged column densities are provided.

To improve the signal-to-noise ratio in the weaker transitions, we smoothed the data to a resolution of 0.5 km s^{-1}. At this resolution, each line has a single-peak Gaussian profile (v_{lsr} = 10.0 ± 0.2 km s^{-1}, Δv = 1.7 ± 0.3 km s^{-1}), while, at the original resolution of 0.12 km s^{-1}, two peaks were detected in the $5_{1,5} \rightarrow 4_{1,4}$ H_2CO and in the $6_{-1} \rightarrow 5_{-1}$ CH_3OH-E transitions. Non-Gaussian profiles were found in other transitions as well. By fitting the $6_{-1} \rightarrow 5_{-1}$ CH_3OH-E line with the GAUSS method of CLASS, we found two velocity components at v_{lsr} = 10.89 ± 0.06 and v_{lsr} = 9.82 ± 0.05 km s^{-1}, with Δv = 0.62 ± 0.13 and Δv = 0.63 ± 0.06 km s^{-1}. These values resemble what LS03 found for the $H^{13}CN$ clumps 1, 5 and 8, which are all within our beam. For the sake of simplicity, one velocity component was used both for the CH_3OH and the H_2CO analysis, as derived from the smoothed CH_3OH data.

High density ($n \sim 7 \times 10^6$ cm^{-3}) and a moderately high temperature ($T \sim 70$ K) are needed to reproduce the CH_3OH spectrum. The temperature is constrained to this value by the non-detection of high-excitation ($E_{low} \geq 80$ K) lines (Fig. 1). The high density value we derived suggests that CH_3OH comes from small clumps. Therefore, guided by LS03, we used a source size of 5″ and derived $N(CH_3OH$-E) = 7×10^{14} cm^{-2} and $N(CH_3OH$-A) = 8 × 10^{14} cm^{-2}. Our estimate of n in the clumps agrees with previous studies (e.g. Young Owl et al. 2000; LS03); T_{kin} is also similar to previous results for the clump gas (see discussion in LS03) and to theoretical models (Gorti & Hollenbach 2002). The

---

[2] http://www.cdms.de
[3] http://spec.jpl.nasa.gov

Table 1. Line parameters of the observed transitions.

Transition	Frequency [MHz]	E_{low} [K]	$\int T_{MB} dv$ [K km s^{-1}]
H_2CO $4_{1,4} \rightarrow 3_{1,3}$	281526.929	32.06	10.7 ± 0.5
H_2CO $4_{0,4} \rightarrow 3_{0,3}$	290623.405	20.96	5.9 ± 0.4
H_2CO $4_{2,3} \rightarrow 3_{2,2}$	291237.767	68.09	2.4 ± 0.3
H_2CO $4_{3,2} \rightarrow 3_{3,1}$	291380.488	126.95	3.4 ± 0.3
H_2CO $4_{3,1} \rightarrow 3_{3,0}$	291384.264	126.95	3.7 ± 0.3
H_2CO $4_{1,3} \rightarrow 3_{1,2}$	300836.635	33.45	9.8 ± 0.5
H_2CO $5_{1,5} \rightarrow 4_{1,4}$	351768.645	45.57	10.1 ± 0.9
CH_3OH-E $6_0 \rightarrow 5_0$	289939.477	47.93	0.5 ± 0.1
CH_3OH-E $6_{-1} \rightarrow 5_{-1}$	290069.824	40.39	0.9 ± 0.2
CH_3OH-A $6_0 \rightarrow 5_0$	290110.666	34.82	1.2 ± 0.2
CH_3OH-E $6_1 \rightarrow 5_1$	290248.762	55.87	0.3 ± 0.2
CH_3OH-E $6_2 \rightarrow 5_2$	290307.376	60.72	0.3^a ± 0.2
CH_3OH-E $6_{-2} \rightarrow 5_{-2}$	290307.643	57.07	
CH_3OH-A $1_1 \rightarrow 1_0$	303366.890	2.32	0.6 ± 0.2
CH_3OH-A $2_1 \rightarrow 2_0$	304208.350	6.96	0.8 ± 0.2
CH_3OH-A $3_1 \rightarrow 3_0$	305473.520	13.93	0.9 ± 0.2
CH_3OH-A $4_1 \rightarrow 4_0$	307165.940	23.21	1.4 ± 0.3
$C^{34}S$ $6 \rightarrow 5$	289209.068	34.70	4.6 ± 0.7
$C^{33}S$ $6 \rightarrow 5$	291485.935	34.98	1.6 ± 0.3
CS $6 \rightarrow 5$	293912.087	35.27	40.7 ± 2.2
CS $7 \rightarrow 6$	342882.850	49.37	33.1 ± 1.9
HCS^+ $7 \rightarrow 6$	298690.453	43.01	0.3 ± 0.1
HCS^+ $8 \rightarrow 7$	341350.229	57.34	0.6 ± 0.1
SO $7_6 \rightarrow 6_5$	296550.064	50.66	3.7 ± 0.5
SO $7_7 \rightarrow 6_6$	301286.124	56.50	4.0 ± 0.6
SO $7_8 \rightarrow 6_7$	304077.844	47.55	7.2 ± 1.3
SO $8_7 \rightarrow 7_6$	340714.155	64.89	3.6 ± 0.7
SO $8_8 \rightarrow 7_7$	344310.612	70.96	3.0 ± 1.1
SO $8_9 \rightarrow 7_8$	346528.481	62.14	7.2 ± 1.2
SO^+ $^2\Pi_{1/2}$ $13/2 \rightarrow 11/2e$	301361.501	38.92	0.6 ± 0.1
SO^+ $^2\Pi_{1/2}$ $13/2 \rightarrow 11/2f$	301736.791	39.03	0.4 ± 0.1
H_2CS $9_{1,9} \rightarrow 8_{1,8}$	304307.645	71.60	0.6 ± 0.1
H_2CS $10_{0,1,0} \rightarrow 9_{0,9}$	342946.335	74.13	0.4 ± 0.1
H_2CS $10_{2,9} \rightarrow 9_{2,8}$	343322.111	126.83	0.4 ± 0.1
H_2CS $10_{1,9} \rightarrow 9_{1,8}$	348534.225	88.47	0.8 ± 0.2
NS $^2\Pi_{1/2}$ $13/2 \rightarrow 11/2e$	299700.097	39.82	0.4 ± 0.1
NS $^2\Pi_{1/2}$ $13/2 \rightarrow 11/2f$	300098.057	39.93	0.4± 0.1
NS $^2\Pi_{1/2}$ $15/2 \rightarrow 13/2e$	345823.532	54.20	0.7 ± 0.2
NS $^2\Pi_{1/2}$ $15/2 \rightarrow 13/2f$	346220.774	54.33	0.8 ± 0.2
H_2S $3_{3,0} \rightarrow 3_{2,1}$	300505.560	154.48	0.5 ± 0.1

^{a} Blended with the $6_{-2} \rightarrow 5_{-2}$ CH_3OH-E line.

H_2 column density (9×10^{22} cm^{-2}) was derived from our observations of the $C^{17}O$(3–2) line, assuming ^{17}O/$^{16}O \sim 1790$ (Wilson & Rood 1994) and T_{rot} = 70 K. The methanol column density then corresponds to a fractional abundance averaged over the beam of 10^{-9}, typical of dark clouds. The 3σ confidence level for T_{kin} ranges between 50 and 75 K, and (5–20) × 10^6 cm^{-3} for n_{H_2}.

The parameters derived from H_2CO differ significantly from the ones of CH_3OH, as high temperature ($T \sim 150$ K) and moderate density ($n \sim 5 \times 10^5$ cm^{-3}) are needed to reproduce the data. Since all H_2CO lines are optically thin, we derived a beam-averaged column density of 9 × 10^{13} cm^{-2} for ortho-H_2CO and 3×10^{13} cm^{-2} for para-H_2CO, corresponding to a fractional abundance of 10^{-9}. Fuente et al. (1996) found the same value, although at another position in the Bar. Our analysis infers a T_{kin} in agreement with the results of Batrla & Wilson (2003) from NH_3, but higher than the one derived by Hogerheijde et al. (1995), 85 ± 30 K, also with formaldehyde, but toward a different position. The density derived is substantially higher than that proposed by Hogerheijde et al. (1995) for the interclump
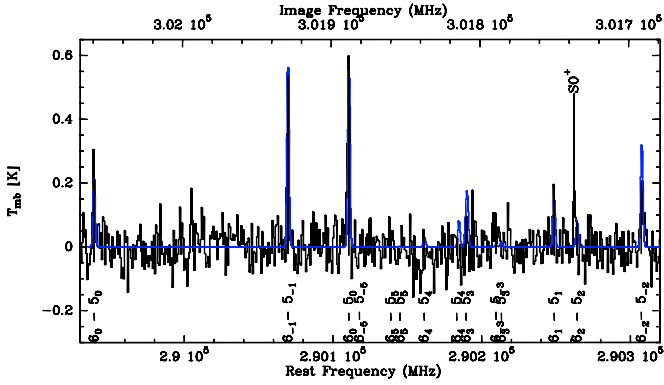
Fig. 1. Spectrum of the $6_k \rightarrow 5_k$ CH$_3$OH band. Overlaid on the data, in blue, is the synthetic spectrum corresponding to our best fit.

Table 2. Column densities of S-bearing molecules.

Species	N [cm^{-2}]	Species	N [cm^{-2}]
NS	$(1.3 \pm 0.3) \times 10^{13}$	SO$_2$	$<3 \times 10^{13}$
SO	$(1.0 \pm 0.2) \times 10^{14}$	HCS	$<4 \times 10^{14}$
SO$^+$	$(2.0 \pm 0.5) \times 10^{13}$	OCS	$<4 \times 10^{13}$
H$_2$S	$(2.5 \pm 1.0) \times 10^{13}$		
H$_2$CS	$(2.5 \pm 0.4) \times 10^{13}$		
HCS$^+$	$(2.5 \pm 0.7) \times 10^{12}$		

medium (3×10^4 cm^{-3}), but it agrees with the value inferred by Simon et al. (1997) based on CN. While the n_{H_2} is well-constrained ($1-5 \times 10^5$ cm^{-3}), the temperature we derived is a lower limit.

The infrared pumping through an internal radiation field would probably affect our results for both molecular species. However, since no model of the IR field is available for the Bar, no internal radiation field was taken into account.

Our data suggest that CH$_3$OH is found mainly in the clumpy medium, while H$_2$CO traces the interclump material. Both methanol and formaldehyde can form on grain surfaces (Watanabe & Kouchi 2002). It therefore seems remarkable that they trace different environments. We speculate that in the interclump gas, methanol, once released from grain surfaces, is photodissociated to form formaldehyde (one of the possible photodissociation products, Le Teuff et al. 2000). Alternatively, our observations may indicate a different formation mechanism for the two species, surface chemistry for CH$_3$OH (as no gas-reaction can efficiently form it, Luca et al. 2002), and gas phase chemistry for H$_2$CO (via the neutral–neutral reaction CH$_3$ + O, e.g. Le Teuff et al. 2000). More detailed modeling, including release of molecules from grain surfaces in the PDR, is clearly needed.

3.2. Sulfur-bearing species

The excitation analysis of the S-bearing molecules listed in Table 1 was performed by fitting all the observed transitions with a synthetic spectrum computed under the LTE assumption, in the manner described by Comito et al. (2005). Since the kinetic temperature, the source size, and the column density are degenerate parameters in the optically thin limit, we fixed T_{kin} to the value derived from H$_2$CO and fit the beam-averaged column density of each species. For SO$_2$, OCS, and HCS, upper limits to the column densities were derived, based on the non-detections of lines in our survey range. Results are given in Table 2. The uncertainties on the column densities are derived with a χ^2 analysis and correspond to the 3σ confidence level. CS and its isotopologs are not included in our analysis, because of the anomalous ^{33}S/^{34}S ratio of $\sim$3 we observed (for comparison, see Chin et al. 1996). Observations of other rotational transitions are needed to constrain this ratio reliably.

Sternberg & Dalgarno (1995, hereafter SD95) studied the chemistry of PDRs produced in a dense molecular cloud exposed to intense far-UV radiation fields. The density they employ ($n_H = 10^6$ cm^{-3}) is higher than the one relevant here for the

interclump gas; discrepancies in the results may be due to this. Their chemical network does not include NS and H$_2$CS, but all the other S-bearing molecules observed here are found there.

According to SD95, the SO$^+$/SO ratio (observed 0.2 from Table 2) can be used as diagnostic of the different chemical zones in the cloud and changes between 0.23 at A_v = 1.5 and 0.0028 at A_v = 3. Assuming that the Bar is edge-on, based on the distance between the ionization front and our position ($\sim$30″), and assuming an H$_2$ density of 10^5 cm^{-3}, we derived a visual extinction of $\geq$10 mag (Frerking et al. 1982). Given the complex geometry of the Orion Bar, which has edge-on (but oblique) and face-on parts (Hogerheijde et al. 1995), it is likely that together with the molecular material at this extinction, a hotter, more diffuse layer of gas, corresponding to a face-on surface layer, contributes to the emission we observe. SD95 predict SO$_2$ to be more abundant than SO and SO$^+$ at high A_v, while our upper limit indicates that SO$_2$ is less abundant. Similar to the result found for SO$^+$/SO, our estimates of SO$_2$/SO and SO$_2$/SO$^+$ suggest that these species have a significant contribution from a hotter layer of gas with lower extinction than the molecular layer.

Fuente et al. (2003) report different column densities for SO$^+$ and SO$_2$; however, their SO$^+$/SO$_2$ ratio ranges between 1.2 at the IR front and 0.4 at (20″, −20″) from it, which is similar to our value of 0.3. Jansen et al. (1995) found values of N(H$_2$S) between 8.9×10^{12} cm^{-2} and 3.9×10^{14} cm^{-2} across the Bar, with our value of 1.3×10^{13} cm^{-2} lying in between. Discrepancies in the absolute values of the column densities may depend on the source sizes, on temperatures, and on the total H$_2$ column density at the observed position.

4. Detection of a deuterated molecule: DCN

Molecular deuteration studies have been extremely powerful in probing the physical history of sources. The deuterium isotopic ratio in molecules can indeed be enhanced in low-temperature environments compared to the cosmic D/H ratio ($\sim$10^{-5}, Linsky 2003). This enhancement proceeds initially from the transfer of deuterium from the main reservoir HD to two reactive ions (H$_2$D$^+$ and CH$_2$D$^+$) through exothermic reactions with H$_3^+$ and CH$_3^+$ (Roberts & Millar 2000, and references therein). The endothermicity of the backward reactions (respectively by 220 K and 370 K) ensures that the H$_2$D$^+$/H$_3^+$ and CH$_2$D$^+$/CH$_3^+$ ratios are significantly enhanced at low temperatures. Deuterium is then channeled to other molecules by gas-phase reactions with these two ions and by grain surface reactions. Highly-deuterated molecules can also be found in hot gas, where they are then out-of-equilibrium fossils of an earlier cold phase (e.g. in hot corinos around low-mass protostars, where they are believed to be remnants of the prestellar cold and depleted chemistry; Parise et al. 2004, 2006).

The DCN(4-3) transition at 289.645 GHz (E_{up} = 34.56 K) was detected in our survey, and found to be very bright (Fig. 2).

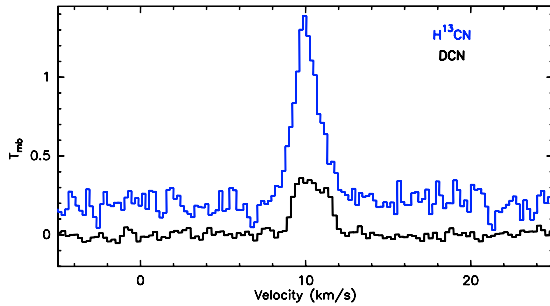**Fig. 2.** $H^{13}CN(4-3)$ and DCN(4−3) lines. For clarity, the $H^{13}CN$ line has been translated by 0.2 along the y-axis.

This detection, together with the detection of DCO^+ in the Horsehead nebula (Pety et al. 2006, in preparation), is opening up the study of fractionation processes in PDRs. The $H^{13}CN(4-3)$ transition (E_{up} = 41.76 K) was also detected at 345.340 GHz. The $H^{13}CN$ emission was shown from interferometric observations (LS03) to be mostly associated with clumps in the PDR. The DCN emission is thus very likely to also be associated with clumps, as DCN would not survive the high temperatures of the interclump gas. The linewidths of DCN(4−3) and $H^{13}CN(4-3)$ are comparable and non-Gaussian profiles are detected in both cases. We thus assume that $H^{13}CN$ and DCN trace the same region. As the energies of the two lines are very similar, the derived abundance ratio is nearly independent of the temperature. Assuming LTE and a $^{12}C/^{13}C$ ratio of 70, we derived beam-averaged DCN and $H^{13}CN$ column densities between 8.4×10^{11} and 1.7×10^{12} cm^{-2}, and between 1.7×10^{12} and 2.8×10^{12} cm^{-2}, respectively, in the range of temperatures 30−150 K. This corresponds to a DCN/HCN ratio of 0.7−0.9%, which is an intermediate value between that observed in warm gas (Orion Hot Core, 0.1%, Schilke et al. 1992), on the one hand, and in dark clouds (L134, 5%, Turner 2001) or cold (30−50 K) gas of the OMC1 ridge region (1−6% Schilke et al. 1992), on the other.

In hot cores/corinos, where the gas has not yet had time to return to equilibrium (which would require timescales of ∼10^4 yr), abundant deuterated molecules can be considered as remnants of earlier cold prestellar chemistry, most probably stored in the ices on grain surfaces and then released when the protostar heats its surroundings. In contrast, the gas in the shielded clumps of the bar might be in steady state. In this case, the observed deuterated molecules have to be present-day product molecules. The detection of DCN in this relatively warm environment, where H_2D^+ would not survive, is in this sense quite striking and is a strong hint of the efficiency of the fractionation processes occurring via the CH_2D^+ channel, which survives higher temperatures than H_2D^+, due to the higher exothermicity of the CH_3^+ reaction with HD (Turner 2001). The Orion Bar thus appears a unique reference to test the fractionation reactions involving CH_2D^+. Knowing the spatial distribution of the DCN/HCN isotopic ratio would then be an interesting tool for understanding the effect of extinction on the fractionation processes.

References

Batrla, W., & Wilson, T. L. 2003, A&A, 408, 231
Chin, Y.-N., Henkel, C., Whiteoak, J. B., Langer, N., & Churchwell, E. B. 1996, A&A, 305, 960
Comito, C., Schilke, P., Phillips, T. G., et al. 2005, ApJS, 156, 127
Frerking, M. A., Langer, W. D., & Wilson, R. W. 1982, ApJ, 262, 590
Fuente, A., Rodríguez-Franco, A., García-Burillo, S., Martín-Pintado, J., & Black, J. H. 2003, A&A, 406, 899
Fuente, A., Rodriguez-Franco, A., & Martin-Pintado, J. 1996, A&A, 312, 599
Gorti, U., & Hollenbach, D. 2002, ApJ, 573, 215
Green, S. 1991, ApJS, 76, 979
Hogerheijde, M. R., Jansen, D. J., & van Dishoeck, E. F. 1995, A&A, 294, 792
Hollenbach, D. J., & Tielens, A. G. G. M. 1997, ARA&A, 35, 179
Jansen, D. J., Spaans, M., Hogerheijde, M. R., & van Dishoeck, E. F. 1995, A&A, 303, 541
Le Teuff, Y. H., Millar, T. J., & Markwick, A. J. 2000, A&AS, 146, 157
Leurini, S., Schilke, P., Menten, K. M., et al. 2004, A&A, 422, 573
Linsky, J. L. 2003, Space Sci. Rev., 106, 49
Lis, D. C., & Schilke, P. 2003, ApJ, 597, L145, LS03
Luca, A., Voulot, D., & Gerlich, D. 2002, in WDS'02 Proceedings of Contributed Papers, Part II, Safrankova (Matfyzpress), 294
Müller, H. S. P., Thorwirth, S., Roth, D. A., & Winnewisser, G. 2001, A&A, 370, L49
Parise, B., Castets, A., Herbst, E., et al. 2004, A&A, 416, 159
Parise, B., Ceccarelli, C., Tielens, A., et al. 2006, A&A, in press
Pety, J., Teyssier, D., Fossé, D., et al. 2005, A&A, 435, 885
Pickett, H. M., Poynter, R. L., Cohen, E. A., et al. 1998, J. Quant. Spectrosc. Radiat. Transfer, 60
Pottage, J. T., Flower, D. R., & Davis, S. L. 2002, J. Phys. B: At. Mol. Phys., 35, 2541
Roberts, H., & Millar, T. J. 2000, A&A, 361, 388
Schilke, P., Pineau des Forêts, G., Walmsley, C. M., & Martín-Pintado, J. 2001, A&A, 372, 291
Schilke, P., Walmsley, C. M., Pineau des Forêts, G., et al. 1992, A&A, 256, 595
Simon, R., Stutzki, J., Sternberg, A., & Winnewisser, G. 1997, A&A, 327, L9
Sternberg, A., & Dalgarno, A. 1995, ApJS, 99, 565, SD95
Störzer, H., Stutzki, J., & Sternberg, A. 1995, A&A, 296, L9
Turner, B. E. 2001, ApJS, 136, 579
Watanabe, N., & Kouchi, A. 2002, ApJ, 571, L173
Wilson, T. L., & Rood, R. 1994, ARA&A, 32, 191
Young Owl, R. C., Meixner, M. M., Wolfire, M., Tielens, A. G. G. M., & Tauber, J. 2000, ApJ, 540, 886